August 27-31, 2023
FLORENCE - ITALY
16th International Conference on Wind Engineering
ICWE 16

Wind field measurements near ground in the Tibetan Plateau

Weizheng Zhou, Wenjuan Lou, Mingfeng Huang

Institute of Structural Engineering, Zhejiang University, Hangzhou, China

SUMMARY:
Currently, there is lacking of research on wind field characterization in the Tibetan Plateau areas. An ultrasonic anemometer was installed at a height of 10 meters above ground in Nagarzê County, Tibet, at an altitude of 4465 m since July 2021, to measure the wind speed and direction continuously. The non-stationary model of wind speed records is established by considering the time-varying mean wind speed. The turbulence intensity, gust factor, integral length scale and wind speed spectrum under the stationary and non-stationary models are respectively analyzed and compared with the results of synoptic winds in other regions with similar topography. The results show that the turbulence characteristics in the plateau differ greatly from other regions, and the non-stationarity of fluctuating winds should be considered when evaluating turbulence characterization at high altitudes especially. The field measurement results provide a reference for the design of buildings and structures in high-altitude plateau areas.

Keywords: plateau, wind field measurement, turbulence characterization

1. INTRODUCTION

The Tibetan Plateau, known as the "Roof of the World", has an average altitude of over 4000 m. The unique plateau climate is influenced by the westerly jet and the southwest monsoon from the Indian Ocean. According to the Chinese load code for the design of building structures, even though the air density in most areas of Tibet is low, the reference wind pressure is still above 0.4 kN/m^2 in most areas of southern and western Tibet, where strong wind occurs frequently. With the economic development of Tibetan, the construction of airports, ultra-high voltage transmission lines, wind farms, and other buildings and structures are steadily advancing. However, current wind field measurements mostly focus on typhoons in coastal area or wind fields of bridges crossing deep gorges (Yu et al, 2019). These wind field measurement results provide little reference for plateau wind fields, and there are few wind field measurements in the Tibetan Plateau, particularly lacking of long-term turbulent wind field measurements. Some studies (Yao et al, 2018) found that wind filed in the plateau shows greatly different from other regions. It is urgent to reveal the wind field characterization in high-altitude plateau areas for wind-resistant design of structures.

2. OVERVIEW OF THE FIELD MEASUREMENTS

A 2D ultrasonic anemometer with a 10 Hz sample frequency was installed at a height of 10 meters above ground in Nagarzê County (W 28°56’40”, E 90°25’00”) at an altitude of 4465m. Nagarzê County has a semi-arid frigid-temperate plateau climate, which is in the south of Tibet. The whole year in Nagarzê can be divided into summer half-year and winter half-year by vernal equinox and autumnal equinox. Fig. 1 shows the surrounding topography of the measurement site, including some low hills, open country, and grasslands. Fig. 2 shows the ultrasonic anemometer.

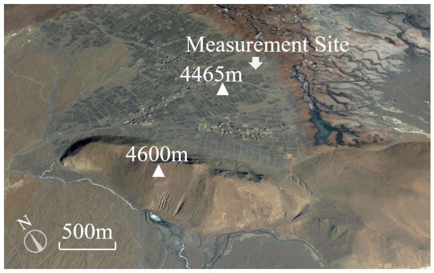

Figure 1. Surrounding topography

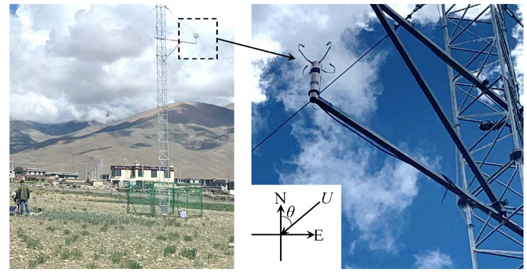

Figure 2. Ultrasonic anemometer

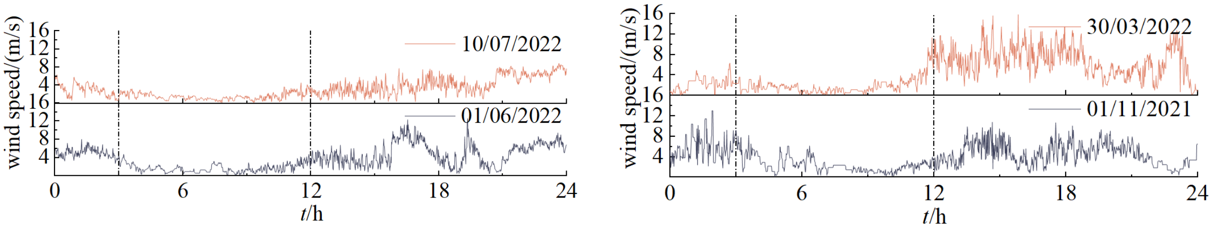

Figure 3. Variation of wind speed in a day

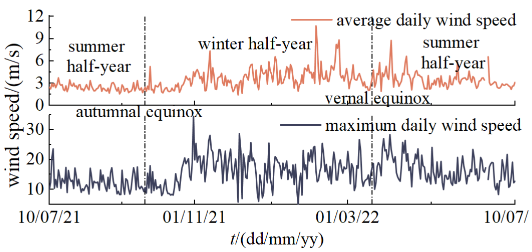

Figure 4. Average and maximum daily wind speed

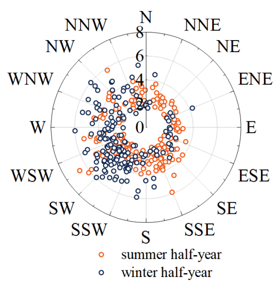

Figure 5. Average daily wind direction

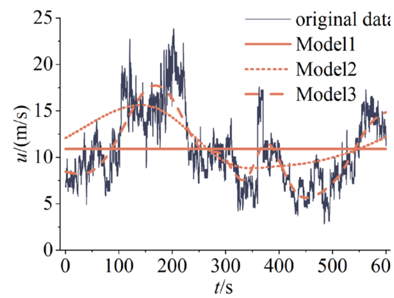

Figure 6. TVM results of different models

Fig. 3 shows several typical 24-hour wind speed and direction variations in the summer half-year and winter half-year. The wind speed is lower from 3:00 to 12:00 and higher from 13:00 to 2:00 due to heated air rising. Fig. 4 shows the average and maximum daily wind speed. Wind speed is greater in the winter half-year. The maximum average and maximum daily wind speed occur in February and November respectively, and there are no significant gale days from July to September. Fig. 5 shows that the wind direction is mainly southwesterly throughout the year.

3. NON-STATIONARY WIND SPEED MODEL

3.1. Vector decomposition of wind speed

The wind speed data are divided into 10-minute samples. The starting time between each adjacent sample is 3 minutes to maximize utilization of wind speed records. Each wind speed sample should be decomposed into longitudinal wind speed u and lateral wind speed v.

3.2. Time-varying mean wind speed

Empirical Mode Decomposition (EMD) method is applied to obtain the time-varying mean (TVM) for establishing non-stationary wind speed models. Model 1 is the stationary model. Table 1 shows three wind speed models analysed in this paper. Fig. 6 shows the result of TVM with a 10-minute record. It could found that Model 3 with more low-frequency components superimposed better represents the trend of non-stationary wind speed.

Table 1. Wind speed models

Case	Model type	Composition of TVM
Model 1	Stationary	Constant mean wind speed
Model 2	EMD	Residual+IMF (end)
Model 3		Residual+IMF (end) +IMF (end-1)

4. RESULTS AND DISCUSSION

Table 2 shows the formulas for different turbulence characteristic parameters. Where σ is the standard deviation, $\bar{u}$ is the mean wind speed over 10-minute, $\max\bar{u}_{t_g}$ is the maximum fluctuating mean wind speed over a time interval of tg=3s, $R_i(\tau)$ is the correction function of fluctuating wind speed.

Table 2. Formulas of different turbulence characteristic parameters

Parameter	Formulas
Turbulence intensity	$I_i = \sigma_i/\bar{u}, (i = u, v)$
Gust factors	$G_u = 1 + \max\bar{u}_{\mathrm{tg}}/\bar{u},\ G_v = \max\bar{v}_{\mathrm{tg}}/\bar{u}$
Integral length scale	$L_i^x = \bar{u}/\sigma_i^2 \int_0^\infty R_i(\tau)d\tau \quad (i = u, v)$

Table 3. Results of measurement compared with synoptic wind in other regions at 10-meter height

Data sources	Altitude /m	Topography	Model	Data period	Range of $\bar{u}$ /(m/s)	I_u	I_v	G_u	G_v	L_u^x/m
Nagarzê in Tibetan Plateau	4465	Plateau	Model1	Sum. half-year	8-15	0.24	0.22	1.58	0.49	246
				Win. half-year	8-12	0.28	0.27	1.72	0.61	249
			Model2	Sum. half-year	8-15	0.21	0.19	1.51	0.43	134
				Win. half-year	8-12	0.25	0.23	1.64	0.55	147
			Model3	Sum. half-year	8-15	0.17	0.16	1.45	0.37	71
				Win. half-year	8-12	0.21	0.19	1.55	0.49	76
Ningxia, China (Huang et al, 2018)	1300	Desert edge	Model1	7-day	5-13	0.19	0.18	1.46	0.34	115
Beijing, China (Li et al, 2013)	500	Grassland	Model1	10-day	5-13	0.18	0.17	1.43	0.38	117
Shanghai, China (Wang et al, 2015)	5	Off the coast	Model1	2-day	3-9	0.28	0.21	1.64	0.46	-

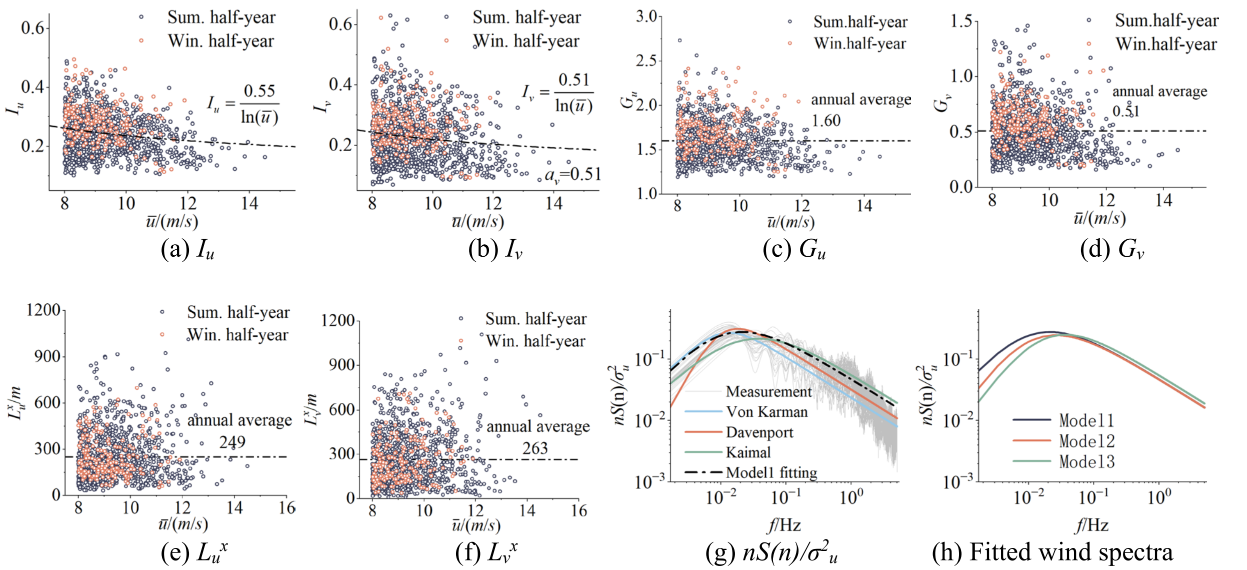

(a) I_u (b) I_v (c) G_u (d) G_v

(e) L_u^x (f) L_v^x (g) $nS(n)/\sigma^2_u$ (h) Fitted wind spectra

Figure 7. Results of turbulence characteristic parameters

Table 3 shows the measurement results compared with other regions. The turbulence characteristic parameters of plateau are higher than the synoptic winds in other regions by Model 1. The integral length scale is particularly large, almost twice as large as in other regions. In Tibetan Plateau, the strong winds during winter half-year show greater values of turbulent characteristics than those during summer half-year. The results in Table 3 obtained by Model 3 are much smaller than the other two models, which indicates that the different non-stationary models might yield different parameter values of turbulence intensity, gust factors and integral length scale.

Fig. 7 presents the results of turbulence characteristic parameters. All parameter values in Fig. 7(a) to 7(f) decrease as the mean wind speed increases. The measured wind power spectra are fitted using the least square method, and the fitted result of measured wind spectra differs from other typical power spectra, as shown in Fig. 7(g). Fig. 7(h) shows that the low-frequency components of fitted wind power spectra of non-stationary models (model 2 and model 3) are lower than that of stationary model, i.e., model 1.

ACKNOWLEDGEMENTS

The research described in this paper was partially supported by the National Natural Science Foundation of China (Project Nos. 51838012 and 52178512).

REFERENCES

Huang, B., Li, Z., Zhao, Z., Wu, H., Zhou, H. and Cong, S., 2018. Near-ground impurity-free wind and wind-driven sand of photovoltaic power stations in a desert area. Journal of Wind Engineering and Industrial Aerodynamics 179, 483-502.

Li, Z., Wu, W. and Wang, Z., 2013. Field measurements of wind characteristics near ground in Beijing suburbs. Journal of Building Structures 34, 82-90.

Wang, X., Huang, P., Dai, Y., and Gu, M., 2015. Comparison study on wind characteristics under typhoon and normal climate conditions in Shanghai area. Journal of Building Structures 36, 93-98.

Yao, Z., Li, X. and Xiao, J., 2018. Characteristics of daily extreme wind gusts on the Qinghai-Tibet plateau, China. Journal of Arid Land 10, 673-685.

Yu, C., Li, Y., Zhang, M.J., Zhang, Y. and Zhai, G.H., 2019. Wind characteristics along a bridge catwalk in a deep-cutting gorge from field measurements. Journal of Wind Engineering and Industrial Aerodynamics 186, 94-104.